SUPPLEMENTAL FIGURE LEGENDS

Supple. Fig. 1. L-PGDS induces directional migration of glial cells. For the checkerboard analysis, migration of mixed glial cells (2 x 10^4 cells/upper well) in response to the indicated concentrations of L-PGDS protein placed in upper and/or lower well was determined using the Boyden chamber assay. The quantification of cell migration was done by enumerating the migrated cells after 24 hr as described under Experimental Procedures. The results are mean ± SD (n = 3) (**A**). A representative microscopic image for each condition is shown (magnification, x100) (**B**).

Supple. Fig. 2. Expression of *l-pgds* in microglia, astrocytes, and neurons. *L-pgds* expression was detected in primary microglia cultures, primary astrocytes, and primary cortical neuron cultures, but not in bEnd.3 endothelial cells, by RT-PCR. β-actin was detected as an internal control. RT (+) and (-) indicate a reverse transcription reaction with or without reverse transcriptase in the RT-PCR analysis, respectively.

Supple. Fig. 3. Effects of recombinant L-PGDS protein on cell viability of microglia and astrocytes. Primary microglia cultures (**A**) or primary astrocytes (**B**) were treated with recombinant L-PGDS protein (1-1,000 ng/ml) for the indicated time periods, and then cell viability was assessed by MTT assay. The results are mean ± SD (n = 3). *$p < 0.05$; compared to the untreated control cells.

Supple. Fig. 4. Polymyxin B has no significant effect on cell migration. Primary microglia cultures (**A**), primary astrocytes (**B**), and NIH3T3 fibroblast cells (**C**) were treated with the mutant L-PGDS protein (100 ng/ml; L-PGDS (C65A)) or wild-type L-PGDS protein (100 ng/ml) in the presence or absence of polymyxin B (10 μg/ml; PB) as indicated. After treatment for the indicated time periods, the wound healing assay was done to evaluate cell migration. A representative microscopic image for each condition is shown (magnification, x100). The results are the mean ± SD (n = 3). *$p < 0.05$ compared to the untreated control (*None*) at the same time point.

Supple. Fig. 5. Pharmacological inhibitors and cell viability. NIH3T3 fibroblast cells were treated with different combinations of PGD_2 (100 ng/ml), recombinant L-PGDS protein (100 ng/ml), C3 transferase (RhoA-specific inhibitor, 0.2 μg/ml), 1L6-hydroxymethyl-chiro-inositol-2-(R)-2-O-methyl-3-O-octadecyl-*sn*-glycerocarbon (Akt-specific inhibitor, 5 μM), SP600125 (Jnk-specific inhibitor, 5 μM), SB203580 (p38-specific inhibitor, 5 μM), and PD98059 (MEK-specific inhibitor, 5 μM) for 24 hr, and then cell viability was assessed by MTT assay (**A**). The results are the mean ± SD (n = 3). NIH3T3 fibroblast cells were treated with recombinant L-PGDS protein (100 ng/ml) in the presence or absence of C3 transferase (RhoA-specific inhibitor, 0.2 μg/ml) for 24 hr, cells were then lysed and subjected to immunoblotting with antibodies against Akt, phosphorylated Akt (Ser-473) (p-Akt), Jnk, or phosphorylated Jnk (p-Jnk) (**B)**.

Supple. Fig. 6. No significant effects of PGD_2 receptor antagonists on cell viability or L-PGDS-induced cell migration. NIH3T3 fibroblast cells were treated with BW A868C (DP1 receptor antagonist, 1-10,000 nM; **A**) and BAY-u3405 (DP2 receptor antagonist, 1-10,000 nM; **B**) for 24 hr, and then cell viability was assessed by MTT assay. The results are the mean ± SD (n = 3). NIH3T3 fibroblast cells were treated with PGD_2 (100 ng/ml) or recombinant L-PGDS protein (10 μg/ml) for 24 hr. Cells were treated with BW A868C (DP1 receptor antagonist, 10 nM) and BAY-u3405 (DP2 receptor antagonist, 10 nM) for 30 min, and then wound healing assay was done to evaluate cell migration (**C**). A representative microscopic image for each condition is shown (magnification, x100).

Supple. Fig. 7. Dose-dependent effects of PGD_2 on cell migration. NIH3T3 fibroblast cells were treated with different concentrations of PGD_2, and then the wound healing assay was done to evaluate cell migration. A representative microscopic image for each condition is shown (magnification, x100).

Supple. Fig. 8. PGD_2-independent effects of L-PGDS on glial cell migration. Mixed glial cells (2 x 10^4 cells/upper well) were treated with BW A868C (DP1 receptor antagonist, 10 nM) and BAY-u3405 (DP2 receptor antagonist, 10 nM) in the presence of PGD_2 (100 ng/ml) or L-PGDS (10 μg/ml), and then Boyden chamber assay was done to evaluate glial cell migration for 24 hr. The quantification of cell migration was

done by enumerating the migrated cells. The results are mean ± SD (n = 3) (**A**). A representative microscopic image for each condition is shown (magnification, x100) (**B**).

Supple. Fig. 9. Role of L-PGDS in astrocyte migration *in vivo*. Following intracortical injection of L-PGDS, the horizontal brain sections were subjected to GFAP immunohistochemistry as described in the Experimental procedures section (**A**). Asterisks indicate the injection sites. For quantification of GFAP intensity, the images were converted into binary images by the NIH image J program. To determine the distribution of GFAP-positive cells, a graticule of 4 concentric circles were drawn with 100 μm intervals using the plugin of the image J program (**B**). Three animals were used for each experimental group. Scale bars, 200 μm.

Supple. Fig. 10. Expression of *marcks* in microglia and astrocytes. *Marcks* expression was detected in primary microglia and astrocytes cultures by RT-PCR. *β-actin* was detected as an internal control. RT (+) and (-) indicate a reverse transcription reaction with or without reverse transcriptase in the RT-PCR analysis, respectively.

Suppl. Fig. 1

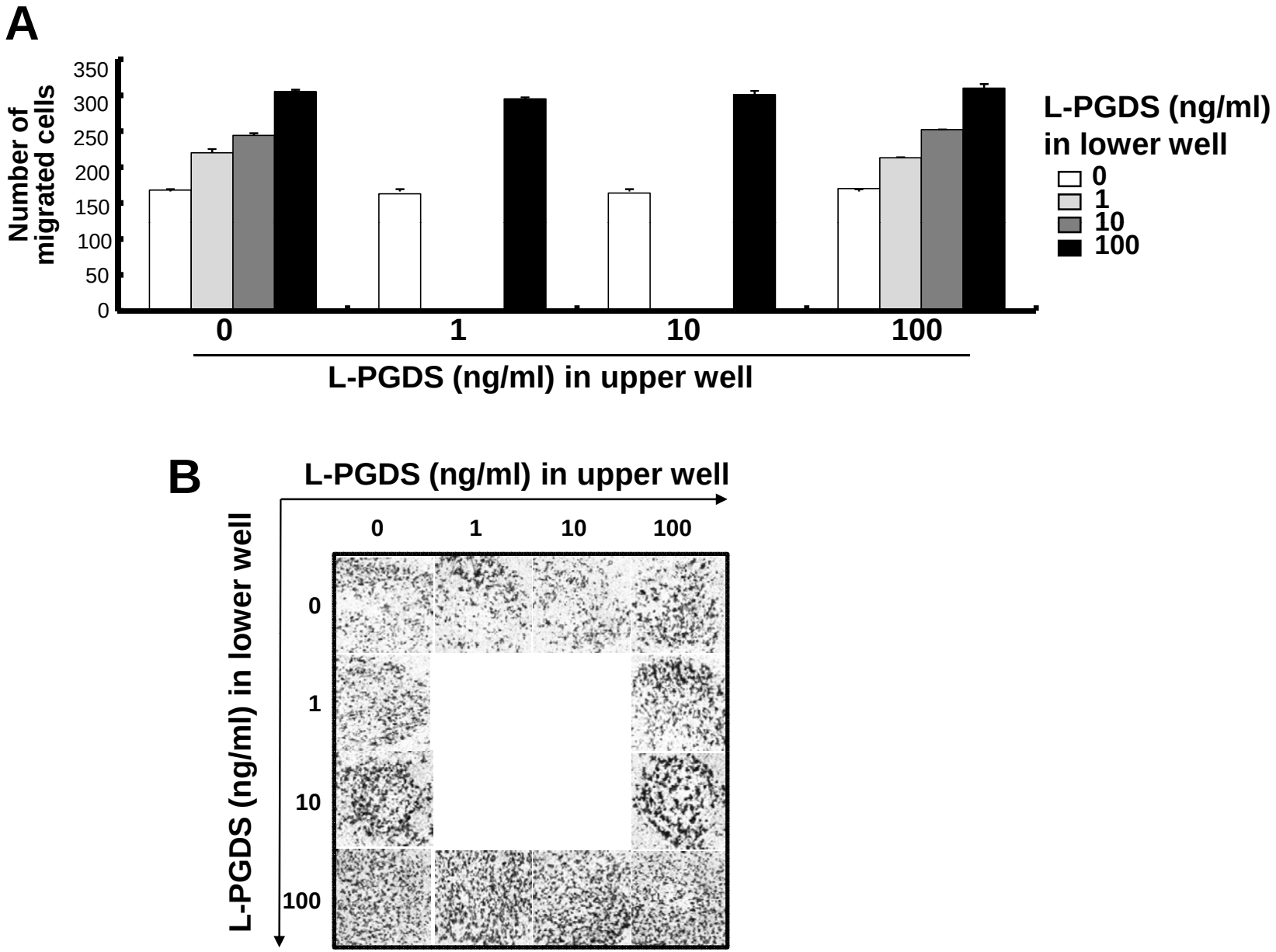
A
Number of migrated cells
350
300
250
200
150
100
50
0
0
1
10
100
L-PGDS (ng/ml) in upper well
L-PGDS (ng/ml) in lower well
0
1
10
100
B
L-PGDS (ng/ml) in upper well
0
1
10
100
L-PGDS (ng/ml) in lower well
0
1
10
100

Suppl. Fig. 2

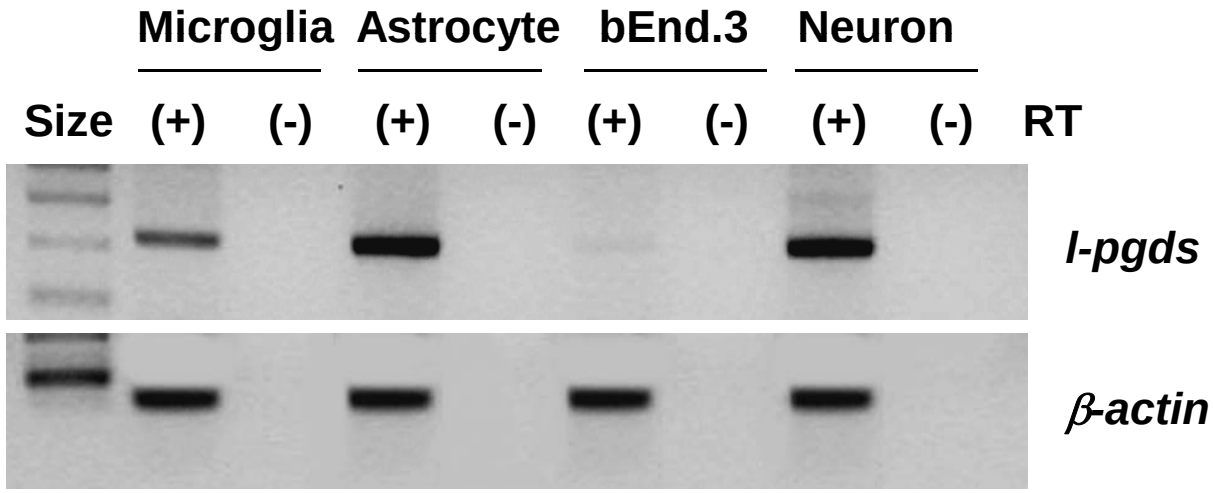

Suppl. Fig. 3

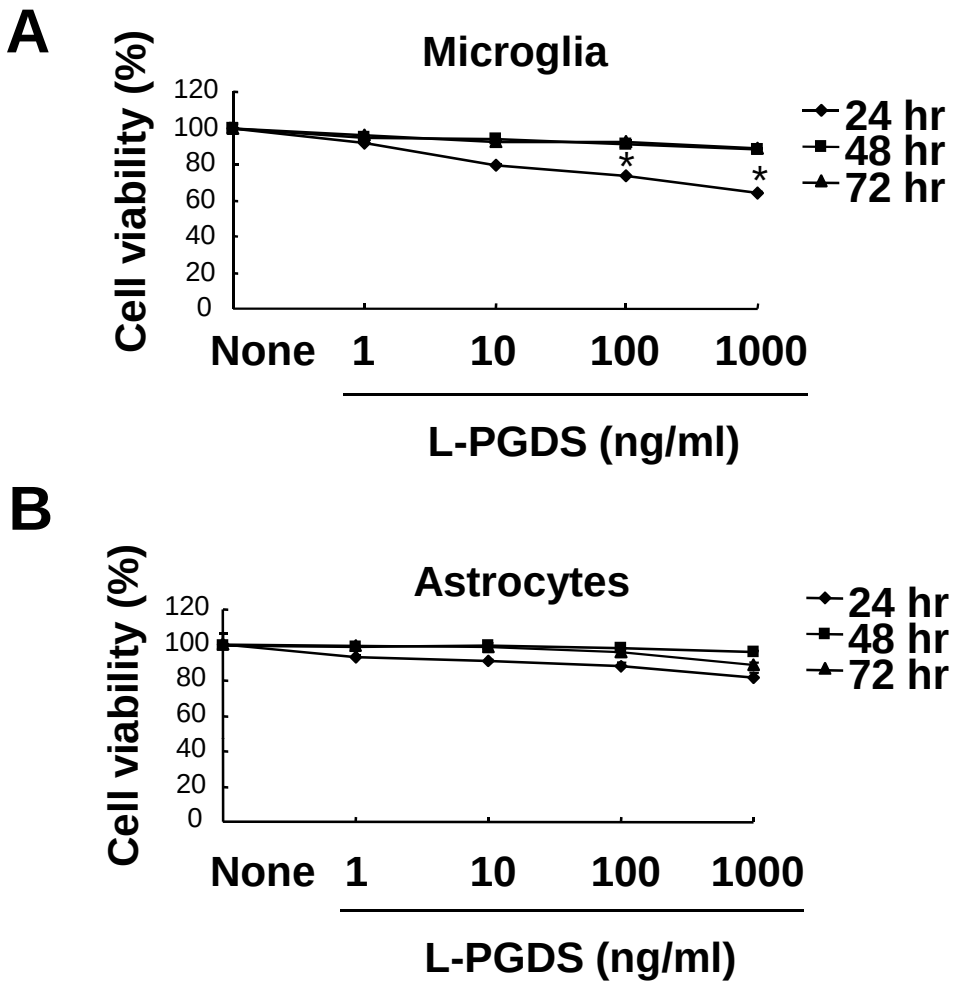
A
Microglia
Cell viability (%)
120
100
80
60
40
20
0
None
1
10
100
1000
L-PGDS (ng/ml)
24 hr
48 hr
72 hr
*
*
B
Astrocytes
Cell viability (%)
120
100
80
60
40
20
0
None
1
10
100
1000
L-PGDS (ng/ml)
24 hr
48 hr
72 hr

Suppl. Fig. 4A, B

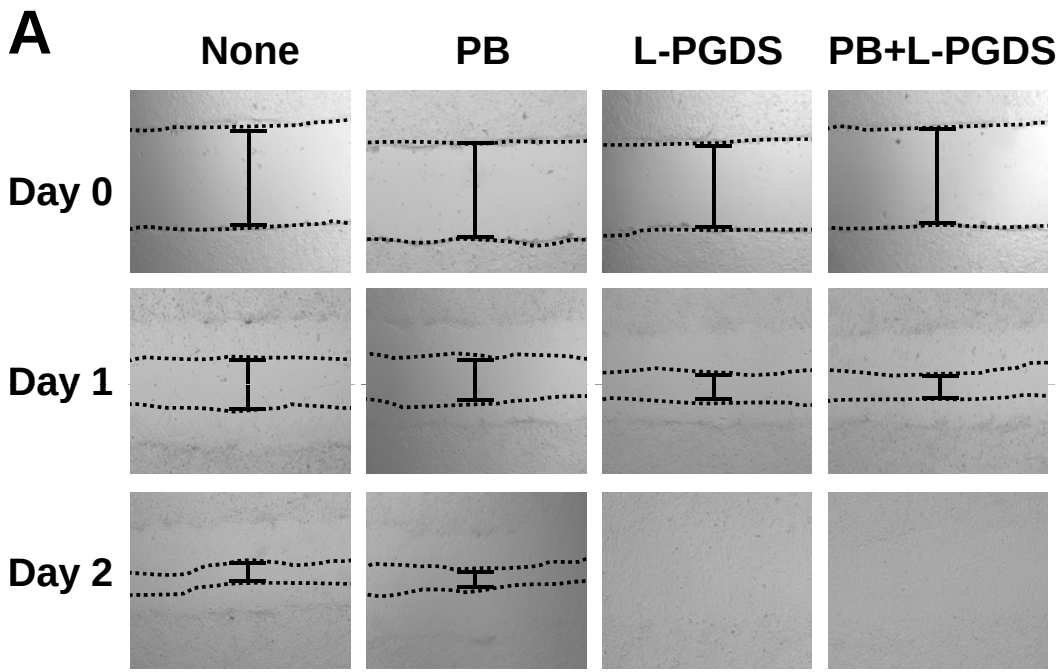

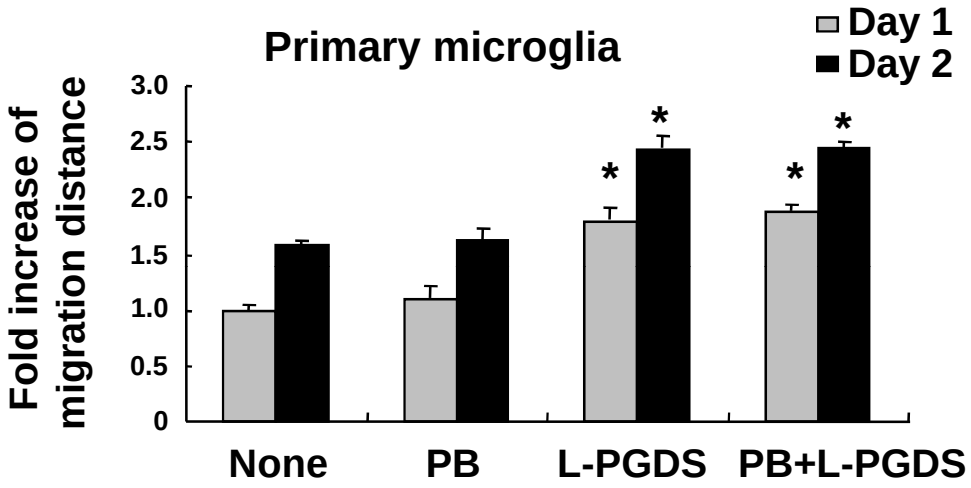

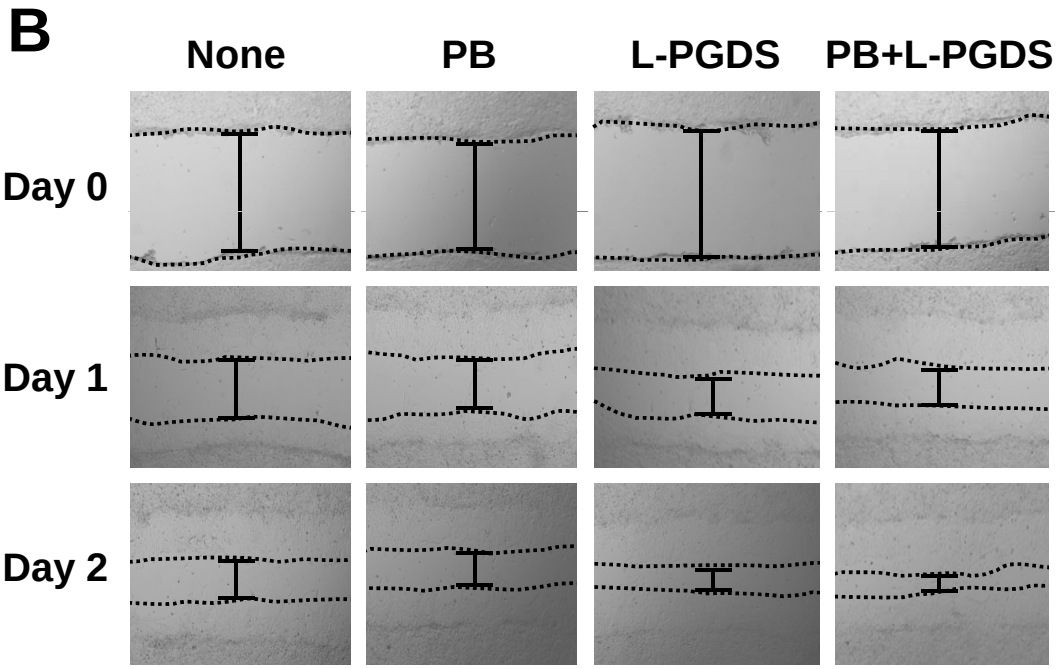

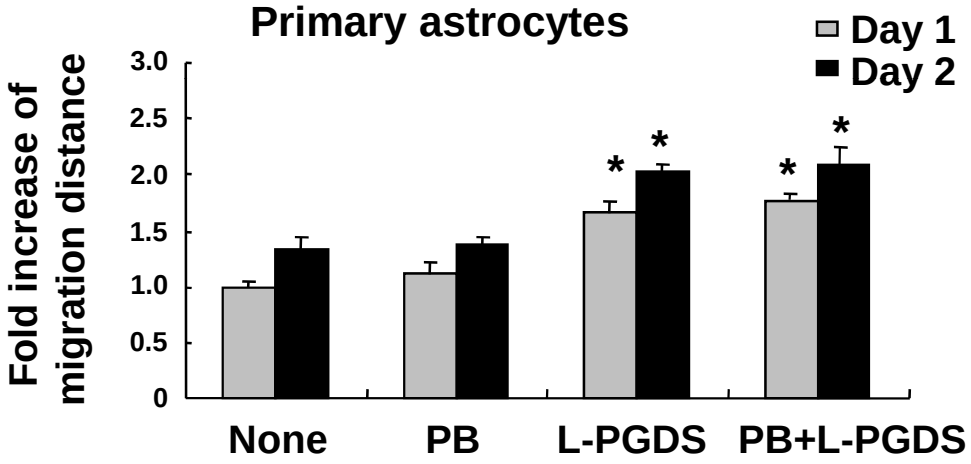

Suppl. Fig. 4C

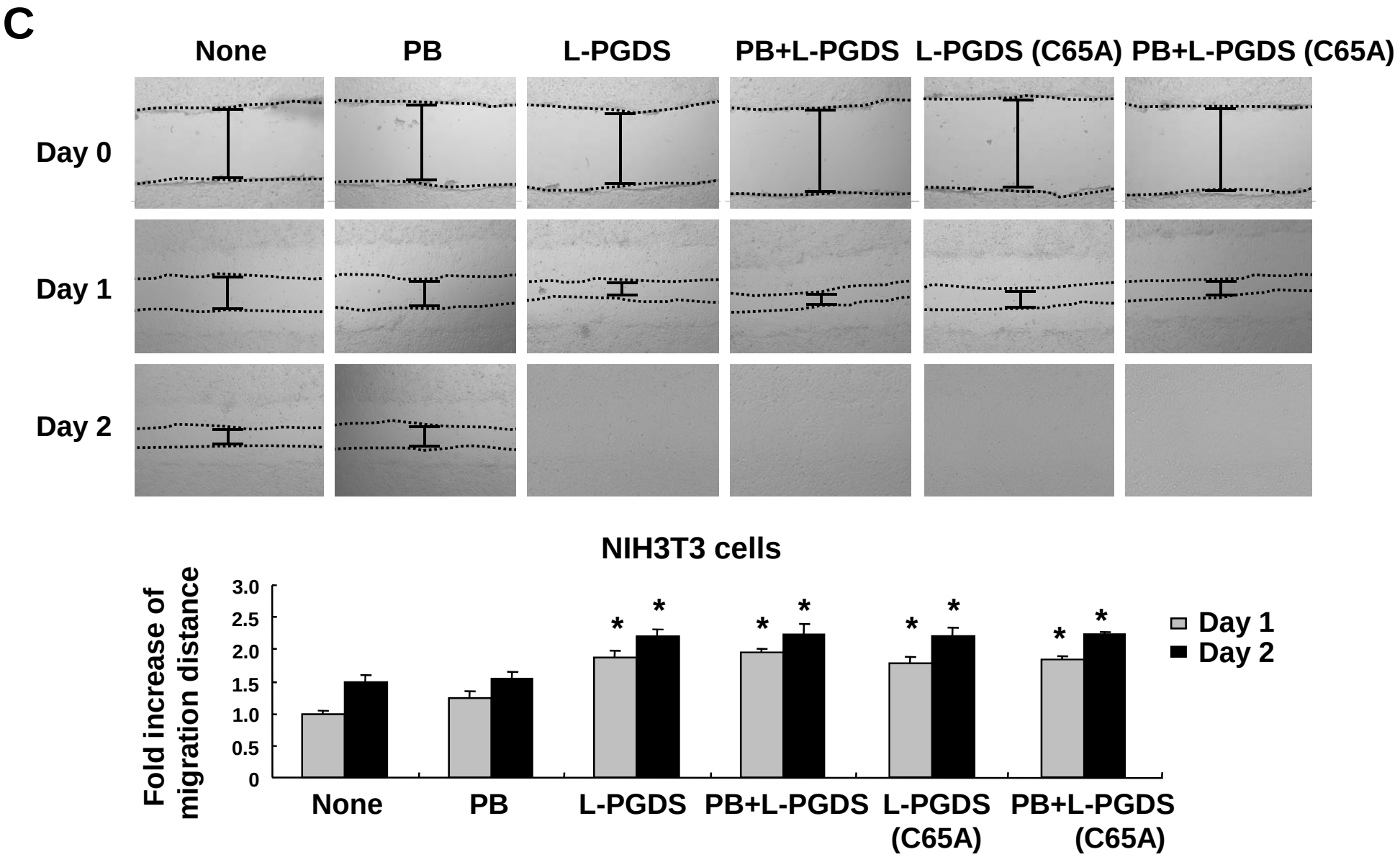
C
None
PB
L-PGDS
PB+L-PGDS
L-PGDS (C65A)
PB+L-PGDS (C65A)
Day 0
Day 1
Day 2
NIH3T3 cells
Fold increase of migration distance
3.0
2.5
2.0
1.5
1.0
0.5
0
*
Day 1
Day 2
None
PB
L-PGDS
PB+L-PGDS
L-PGDS (C65A)
PB+L-PGDS (C65A)

Suppl. Fig. 5

A

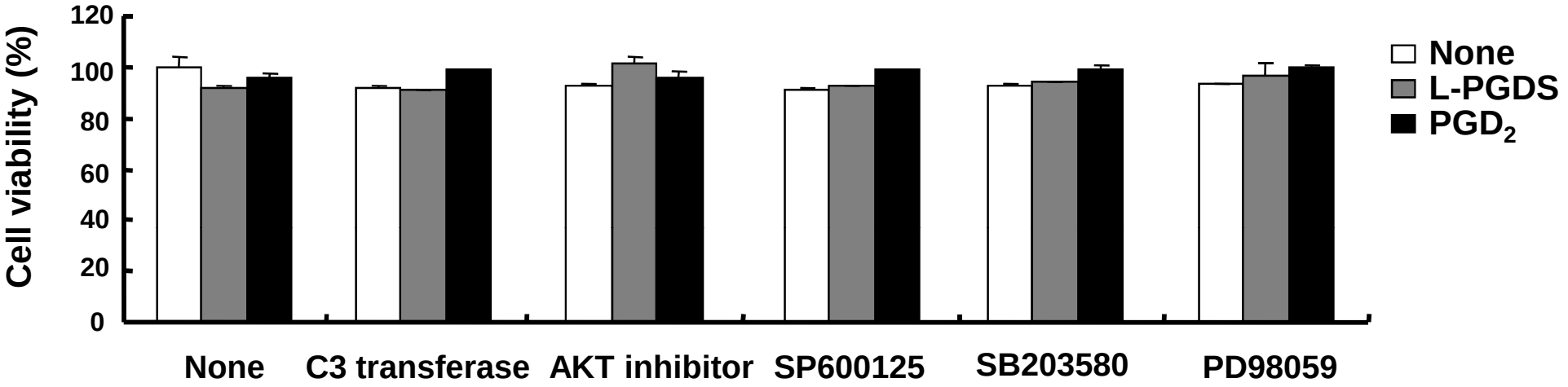

B

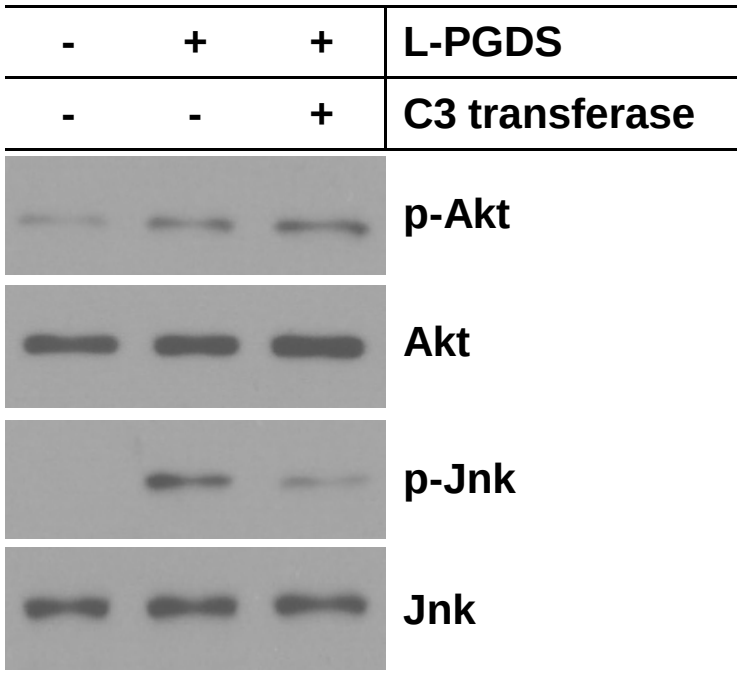

Suppl. Fig. 6A, B

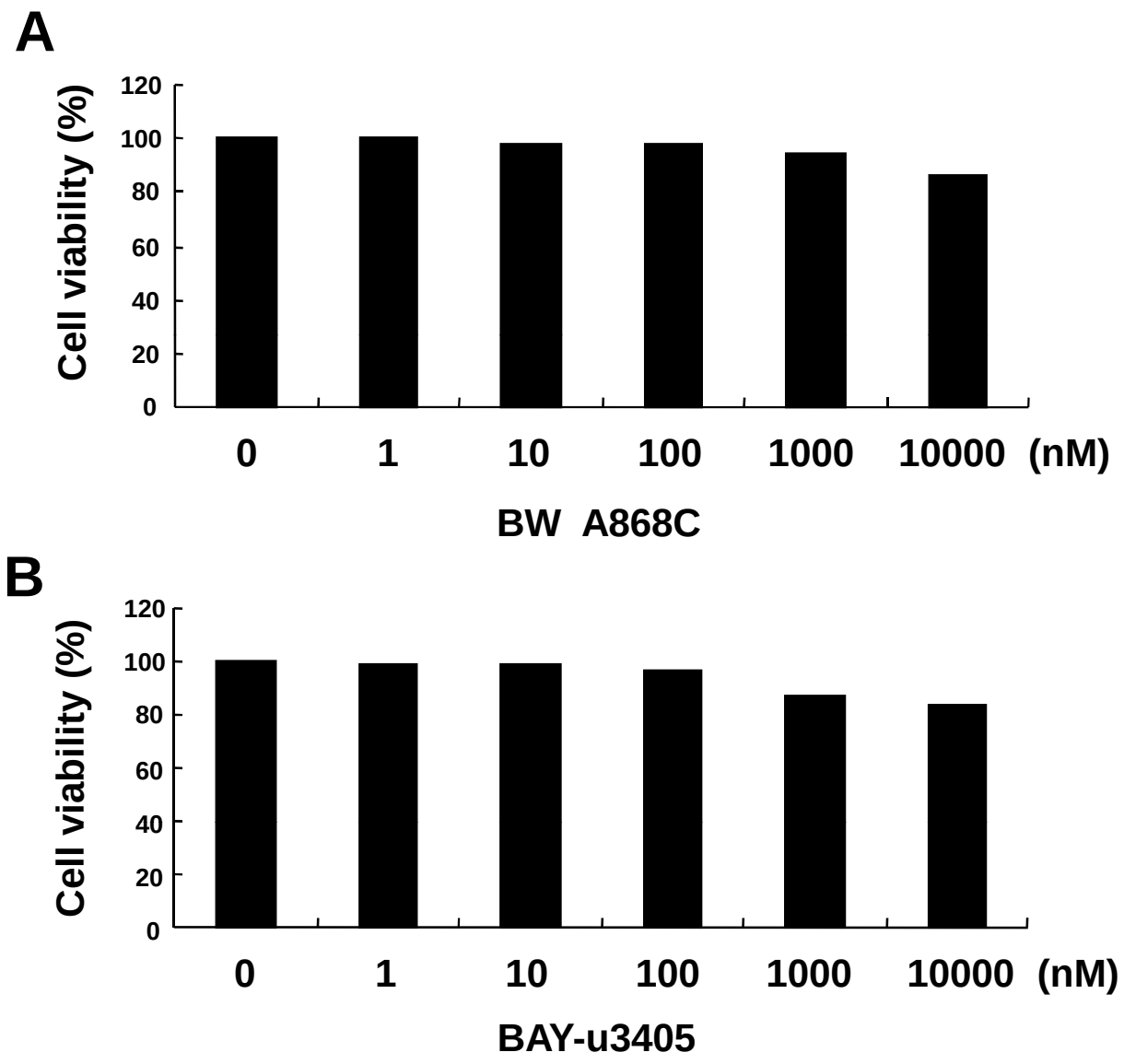

Suppl. Fig. 6C

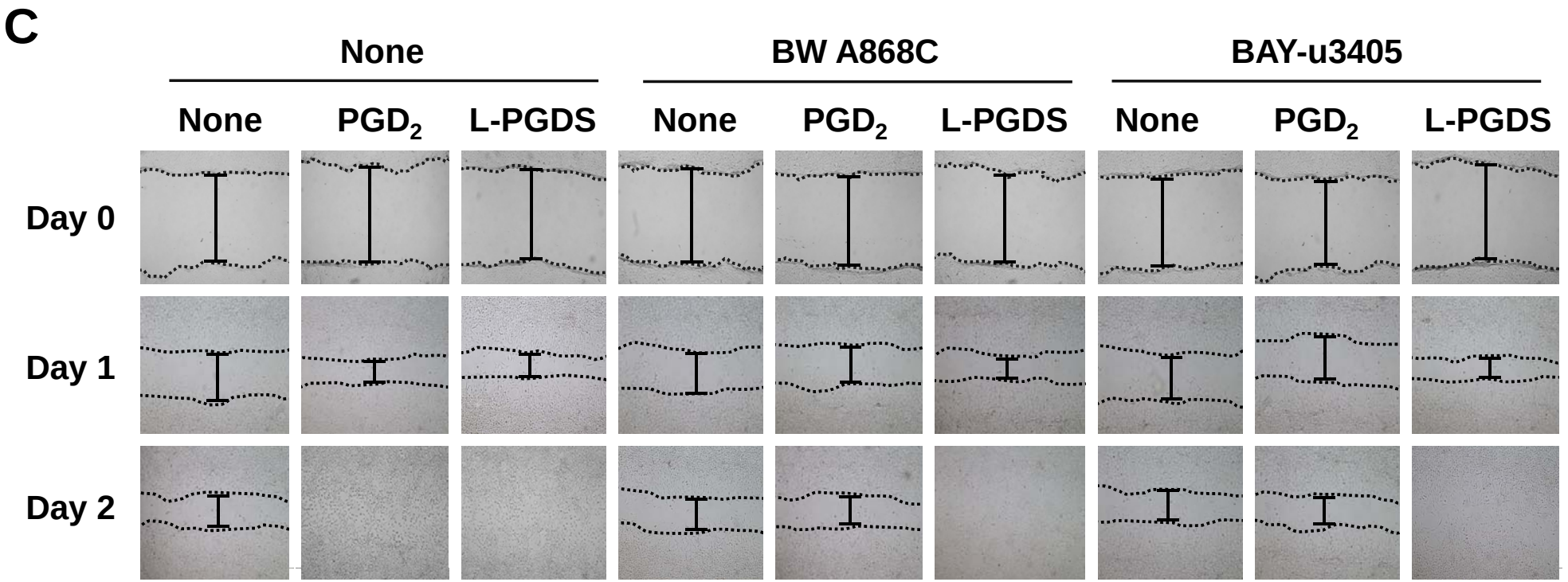
C
None
BW A868C
BAY-u3405
None
PGD2
L-PGDS
None
PGD2
L-PGDS
None
PGD2
L-PGDS
Day 0
Day 1
Day 2

Suppl. Fig. 7

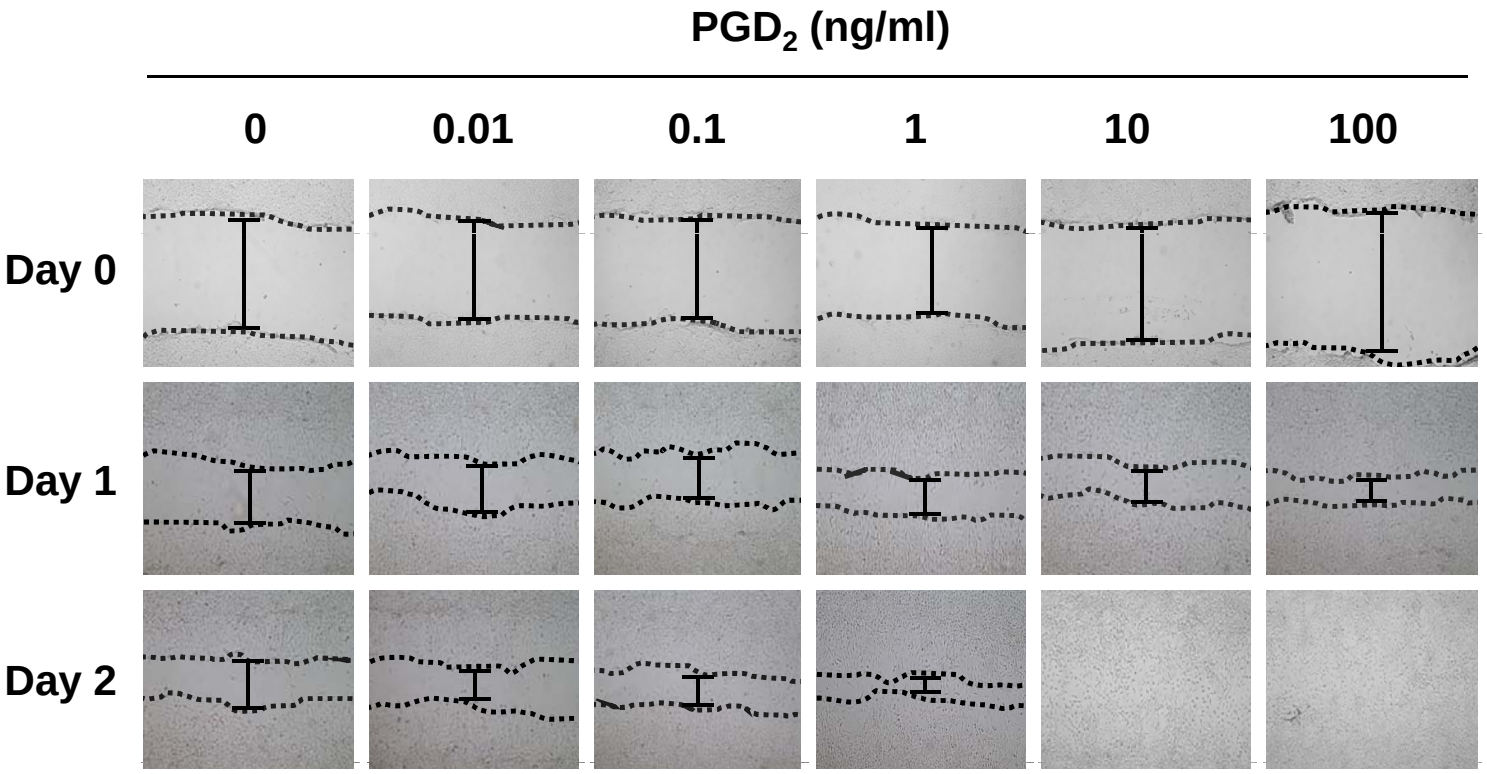

Suppl. Fig. 8

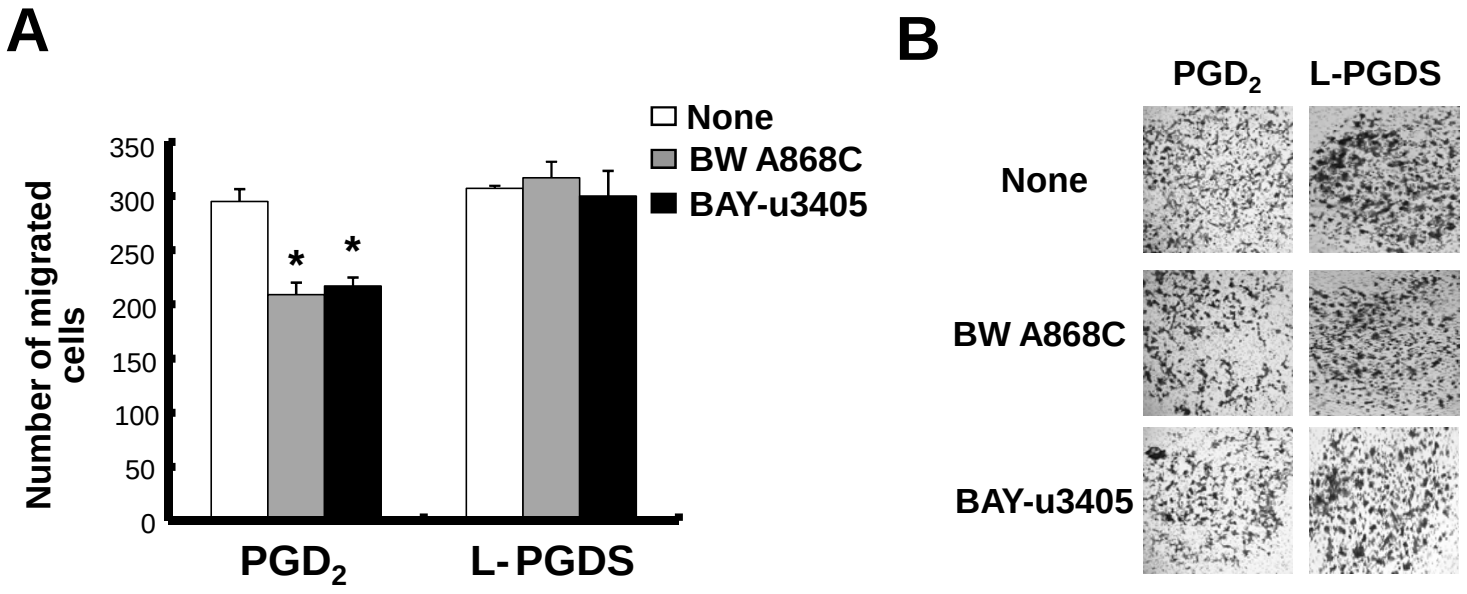
A
Number of migrated cells
350
300
250
200
150
100
50
0
*
*
None
BW A868C
BAY-u3405
PGD2
L-PGDS
B
PGD2
L-PGDS
None
BW A868C
BAY-u3405

Suppl. Fig. 9

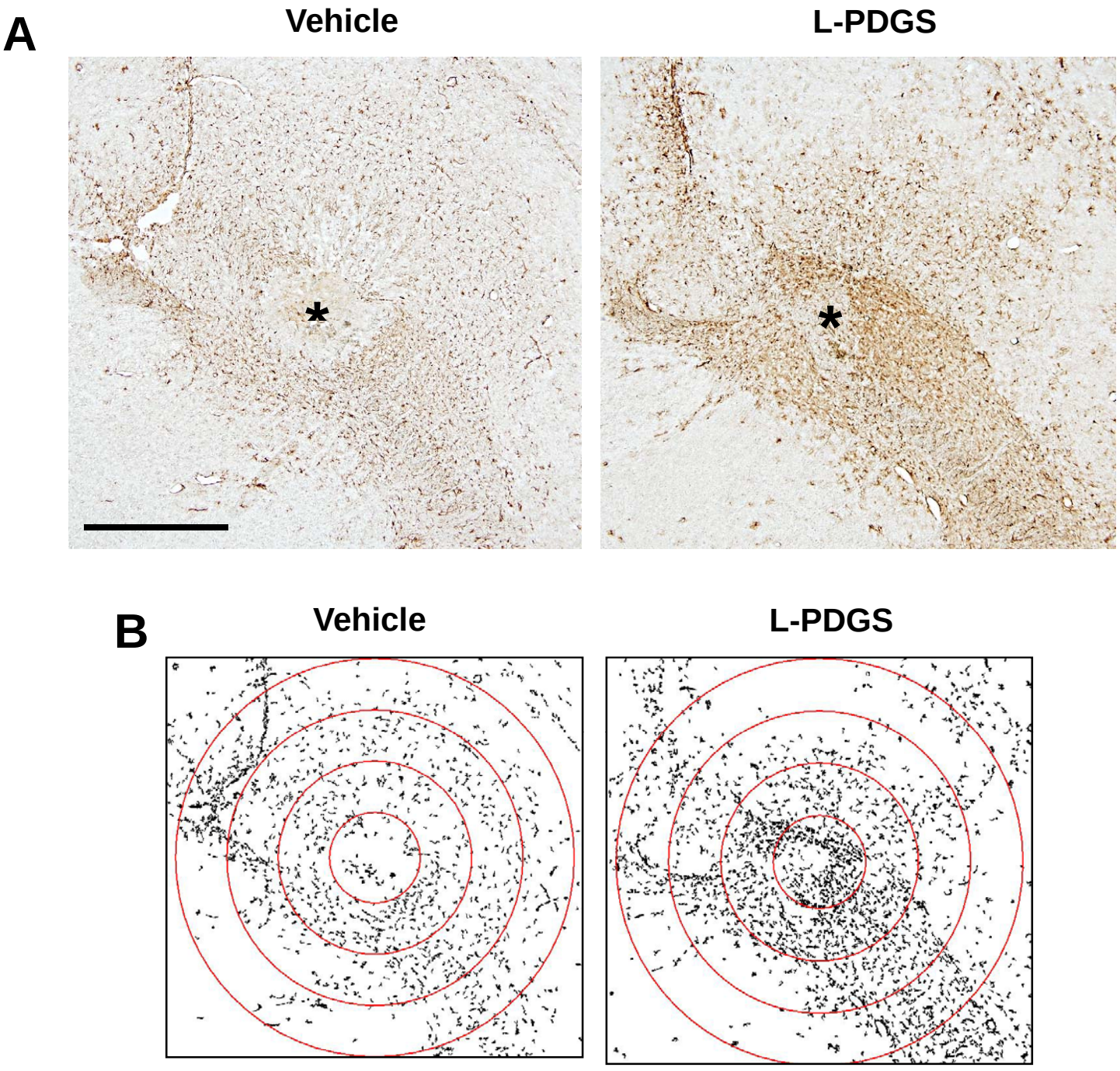
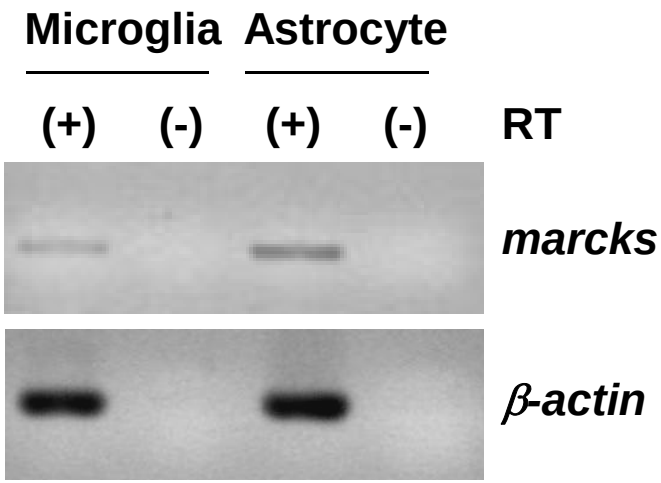
Suppl. Fig. 10